4.
MULTI-BAND SHORTED MONOPOLE ANTENNA FOR HANDSET APPLICATIONS

4.1 Introduction

With technological advancements in wireless communication, the size and weight of mobile handsets have rapidly been reduced. As a result, antennas have gone from external component to internal, becoming subject to numerous constraints in size and function. Earlier, in mobile handsets, multiple antennas (internal and external) are used for different communication applications. In today's scenario there exist lots of communication protocols for different applications like GSM, LTE, WLAN, WiMAX, etc. Therefore, multi-band antennas with broadband capabilities having compact size and easy to fabricate with existing electronics circuitry of the devices, are demanding for now-a-days high end mobile terminals. Many types of antennas are proposed to meet such requirements like inverted-F antenna (IFA) [Chiu and Chi (2009), Soras *et al.* (2002), Lee and Sung (2014)], planar inverted-F antenna (PIFA) [Rhyu *et al.* (2009), Du *et al.* (2003), Yeh *et al.* (2003)], folded chip antennas [Chi and Wong (2008), Peng *et al.* (2011), Li and Wong (2008), Chi and Wong (2009), Hsu and Wong (2009)], meandered line antenna [Bharti *et al.* (2014), Chen and Peng (2011), Dou and Chia (2000), Lung *et al.* (2003)], and monopole antennas [Wong *et al.* (2003), Lee and Wong (2005)]. However, it is difficult to achieve broadband characteristics with compact and planar geometries, using IFA, PIFA, and folded chip antennas. Multi–arm quarter wavelength monopole antennas are good candidate for mobile terminals with broadband and multi-band capabilities. Further, shorting arms can be added to monopole antennas to improve the impedance bandwidth performance of the antenna [Yeh *et al.* (2003)] as well as achieve compact size. Therefore, shorted monopole antenna with planar structure can be very good candidate for slim mobile handsets.

In view of the above, in the present chapter effort is made to further widened the GSM 900 band to achieve the GSM 850 band along with GSM900/

GSM1800/GSM1900/UMTS/ IMT2100/ WLAN/ LTE2500/WiMAX frequency bands along with all the higher LTE (Long Term Evolution) frequency bands by maintaining the same size of the antenna as well as mobile circuit board which was considered in the previous chapter 3. In this connection, a novel compact planar shorted monopole antenna of size 15×50 mm^2 is proposed which is printed on the no ground portion of PCB for slim mobile phones. The proposed planar antenna consists of three branches namely, C-shaped, meandered line, and shorting strip. The proposed antenna covers GSM850/900/1800/1900, UMTS, Wi-Fi, LTE2300/2500, and WiMAX frequency bands.

4.2 Antenna Configuration and Design Evolution

The configuration of the proposed antenna along with fabricated prototype is shown in Fig 4.1(a). The detail dimensions of the antenna are shown in Fig 4.1(b). The proposed antenna fed by 50 Ω microstrip line is printed on the no ground portion of size 15×50 mm^2 on one side of the mobile circuit board of size 50×95 mm^2 whereas the ground plane is printed on the opposite side of the board. The mobile circuit board is made of low cost FR4 substrate with dielectric constant 4.4 and loss tangent 0.018 whereas thickness of substrate is 0.8 mm.

The evolution of the antenna starts with considering four different cases including C-shaped branch only (Case 1), meandered line branch only (Case 2), combination of C-shaped and meandered line branch (Case 3), and PIFA (proposed antenna) as shown in Fig 4.2. The length of the C-shaped branch is chosen λ/4 at 1.8 GHz which is lower edge operating frequency of Case 1. In Case 2, only modified meandered line generates the lower resonant frequency corresponding to the 3λ/8 length [Du *et al.* (2003)] at 0.97 GHz frequency. But the independent operation of meandered line fails to achieve the desired operating frequency bands at lower frequency side as well as higher frequency side due to narrow bandwidth. To achieve the wideband operation of the antenna, C-shaped branch and the meandered line branch is joint together which results in wideband frequency of operation covering 1.7 GHz to 2.03 GHz with some mismatched around 2.1 GHz at higher frequency side. Still the most operational frequency

bands i.e. GSM850/900 and WiMAX frequency bands are not covered with this configuration.

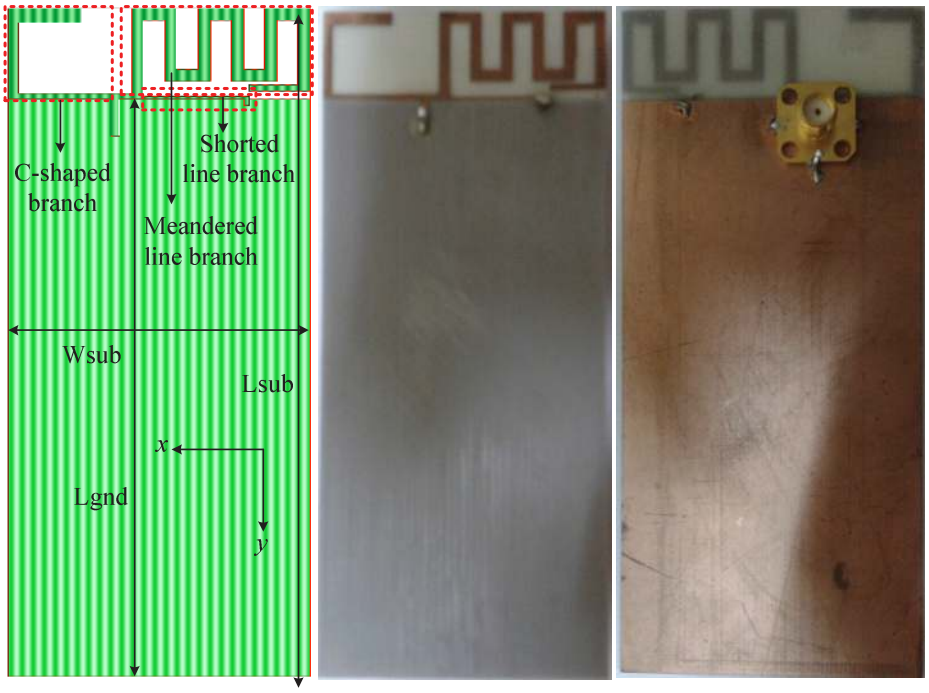

(a)

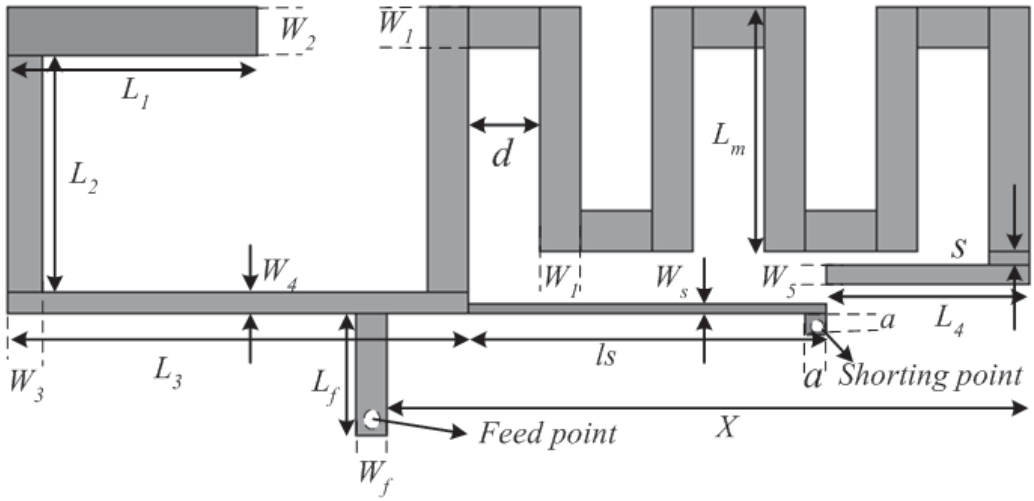

(b)

Fig. 4.1: Configuration of proposed antenna, (a) Configuration along with fabricated prototype and (b) Detail dimensions of the antenna element.

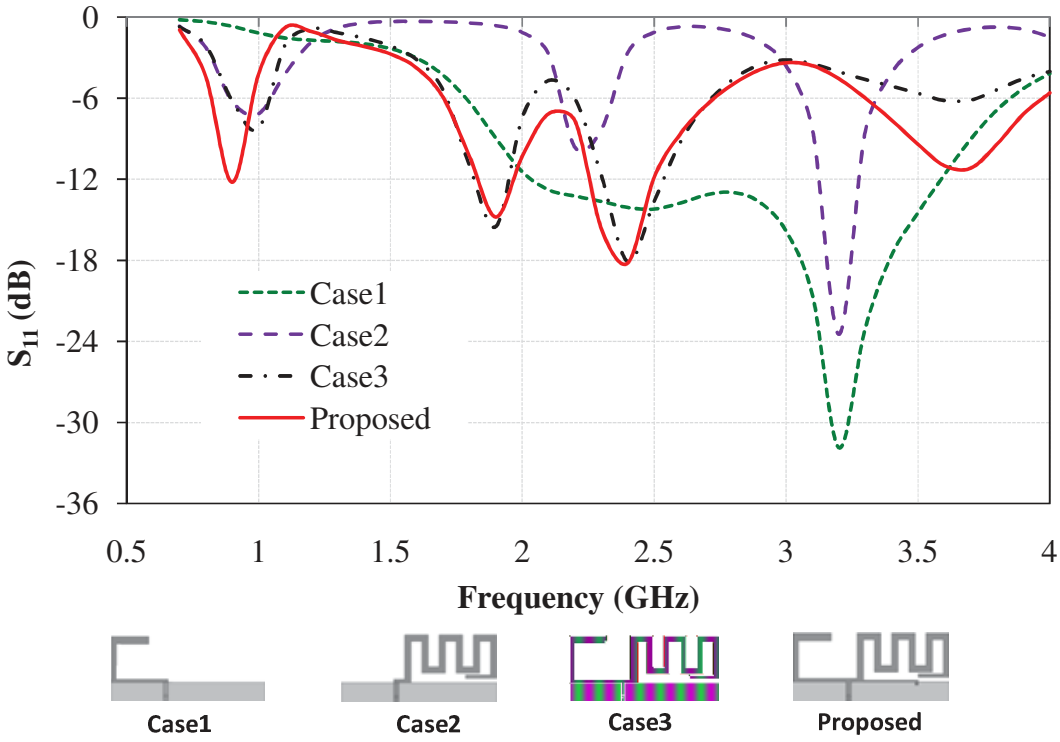

Fig. 4.2: Effect of different configuration on reflection coefficient.

It is highly desirable to achieve GSM850/900 bands and WiMAX band along with other communication bands which are utilized in modern mobile handsets. Therefore, to achieve the aforesaid frequency bands, shorting strip of λ/4 length at 3.5 GHz is connected with antenna considered in Case 3 as shown in Fig 4.1. Due to the shorting strip, significant amount of electrical length of the meandered line branch increases hence the lower resonant frequency decreases (Fig. 4.2) and WiMAX band (3.3 GHz–3.7 GHz) is also covered. It is also observed that the impedance matching is improved around 2.1 GHz, hence wideband (1.7 GHz–2.03 GHz) frequency of operation is achieved.

All the simulations are carried out using finite element method (FEM) based Ansoft high frequency structure simulator (HFSS) to optimize the shape parameters of the antenna to achieve the desired wideband of operation. The

simulated HFSS results are validated by finite integration technique (FIT) based computer simulation technology microwave studio (CST MWS) and measured results. Further, CST MWS is used to study the SAR in human head phantom placed in the vicinity of the proposed antenna. The optimized shape parameters of proposed antenna are shown in Table 4.1.

4.3 Antenna Characterization in Free Space

The simulations are performed originally in Ansoft's HFSS to optimize the antenna parameters for the desired operating bands.

4.3.1 S-Parameter Characterization

In this section *S*-parameter of the proposed antenna is investigated for the different shape parameters to see the effect on the impedance bandwidth. Thereafter, the simulated results are compared with the measured result.

Table 4.1: Optimized shape parameters of the proposed antenna.

Parameters	**Value (mm)**	**Parameters**	**Value (mm)**
Wsub	50	L_m	12
Lsub	110	W_1	2
Lgnd	95	W_2	2.4
L_1	12.2	W_3	1.7
L_2	11.6	W_4	1
L_3	17	W_5	1
L_4	10	W_s	0.5
L_f	6	W_f	1.5
l_s	17.5	S	0.6
X	31.5	d	3.5
Feed point	(32.25,19.5)	a	1
Shorting point	(10.5, 15.5)		

4.3.1.1Parametric analysis

Parametric study of some critical dimensions/shapes of the antenna is carried out to analyze the effect of the shape parameters on the operating frequency bands using HFSS. The antenna is designed to cover the GSM 850/900/1800/1900/ UMTS/ IMT 2000/ WLAN/ WiMAX and higher LTE bands.

The effect of variation of length of one arm of C-shaped branch L_1 on impedance bandwidth is shown in Fig 4.3. It is observed that with the increase of the length L_1, resonant frequency decreases rapidly around 2 GHz and 2.4 GHz whereas it is almost unaffected around GSM 850/900 band. The impedance bandwidth ($S_{11} \leq -6$ dB) of higher frequency does not get affected significantly, but the impedance matching around 3 GHz and 2.7 GHz reduces while impedance matching about 2 GHz gets improved. Since the length of quarter wavelength C-shaped strip is responsible for resonating mode around 2 GHz, shifting of resonant frequency around 2.4 GHz towards lower frequency takes place while mismatch occurs around 3.5 GHz.

The effects of variations of W_2, W_3, and W_4, on impedance bandwidth are shown in Figs. 4.4, 4.5, and 4.6, respectively. It is observed that with the effect of variation of width W_2 and W_3 on impedance bandwidth is very less significant at overall frequency band while more prominent matching effected is observed near 1.9 GHz, 2.4 GHz, and 3.5 GHz. While W_4 affect the higher frequency band significantly as it is directly fed by feed line and with increase of W_4 impedance matching improve significantly at higher frequency side. Since these width are related to C-shaped branch therefore lower frequency band is not affected.

The effects of variations of feed position X and length of shorting strip l_s on the impedance bandwidth are shown in Figs. 4.7 and 4.8, respectively. It is observed that both the lower and higher frequency bands are affected due to variation of these parameters. With the increase of X and l_s the impedance matching towards higher frequency side improves significantly, while the lower frequency band shifted towards lower values.

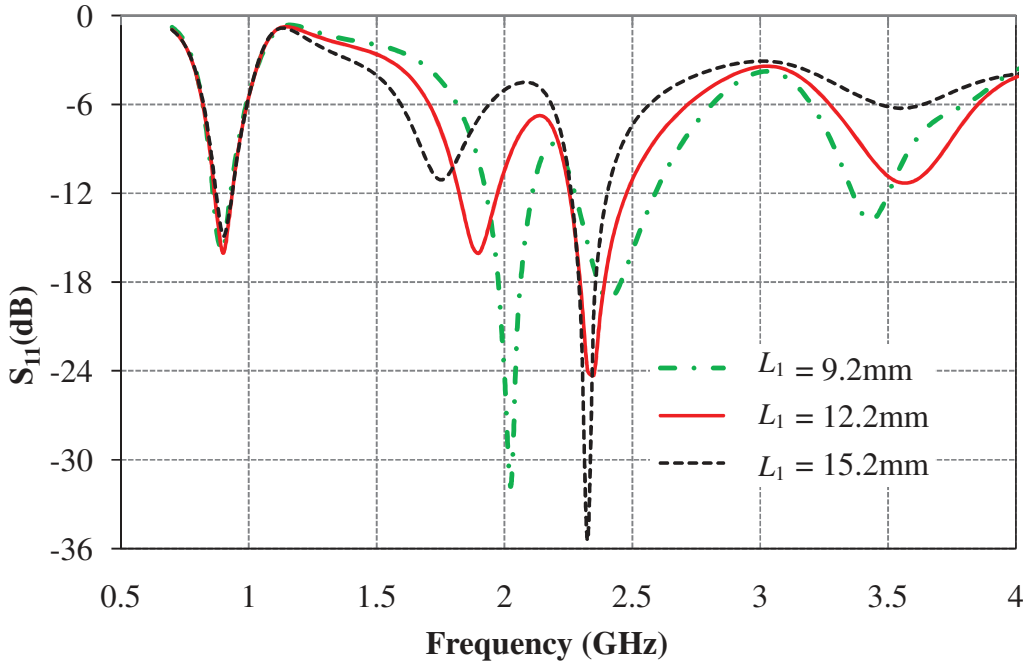

Fig. 4.3: Variation of reflection coefficient with frequency for length L_1.

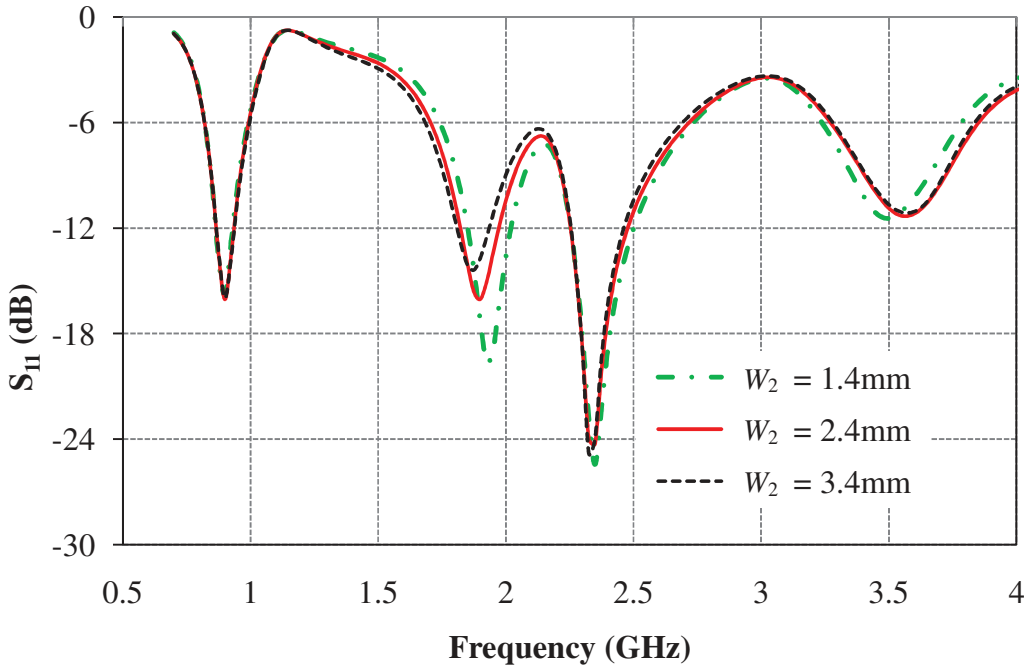

Fig. 4.4: Variation of reflection coefficient with frequency for width W_2.

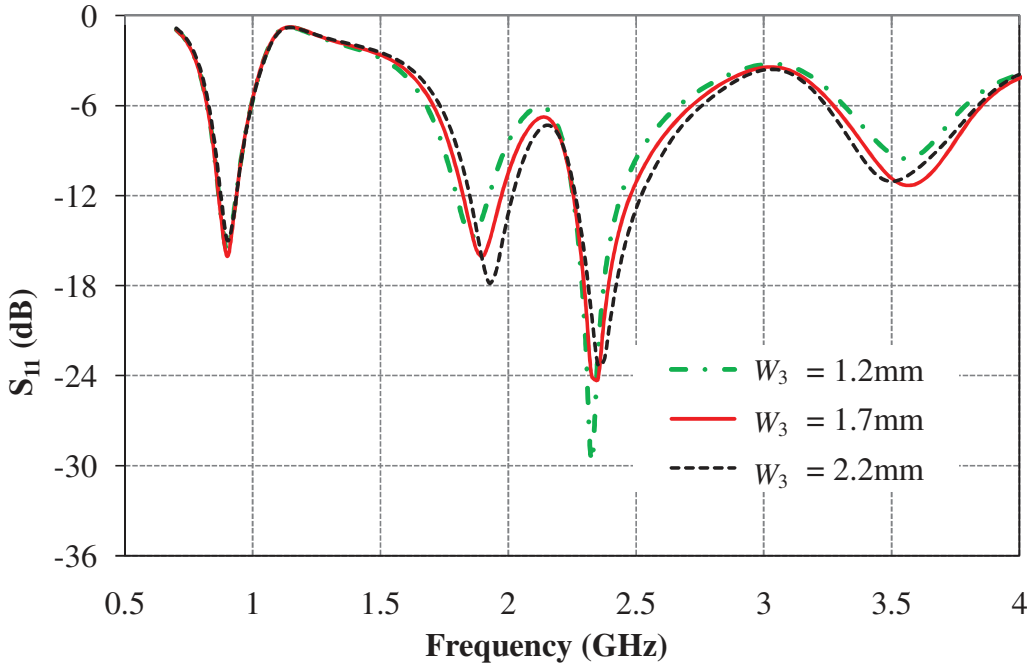

Fig. 4.5: Variation of reflection coefficient with frequency for width W_3.

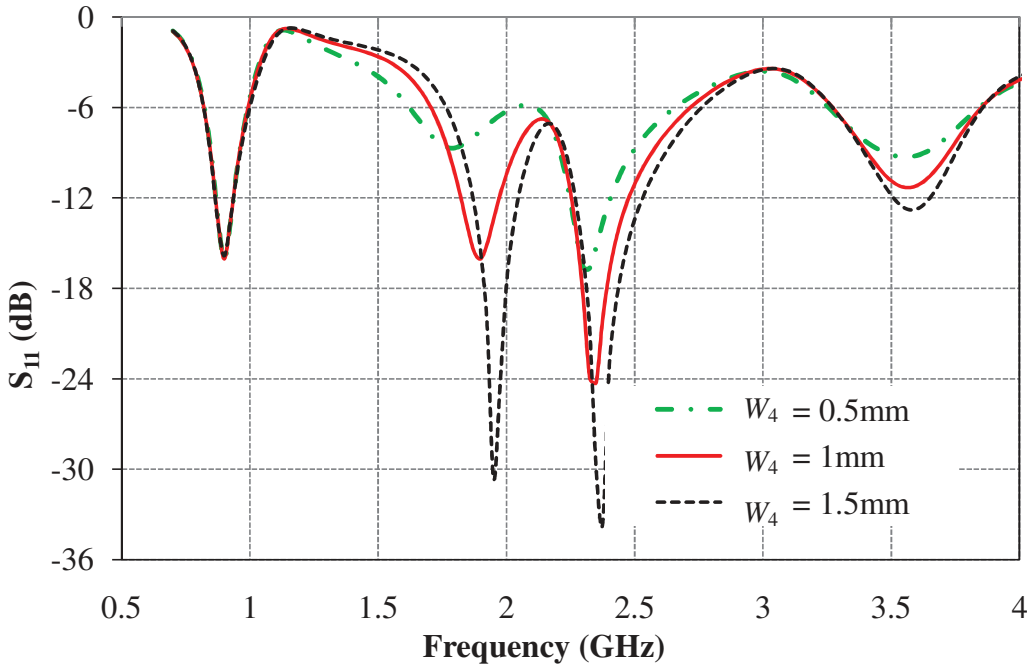

Fig. 4.6: Variation of reflection coefficient with frequency for width W_4.

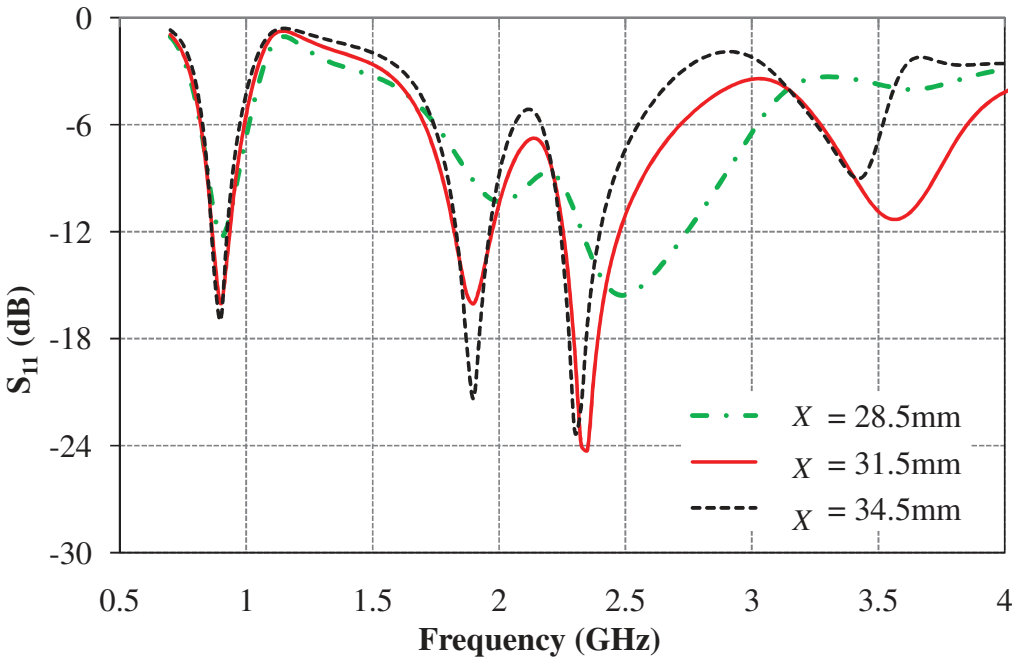

Fig. 4.7: Variation of reflection coefficient with frequency for *X*.

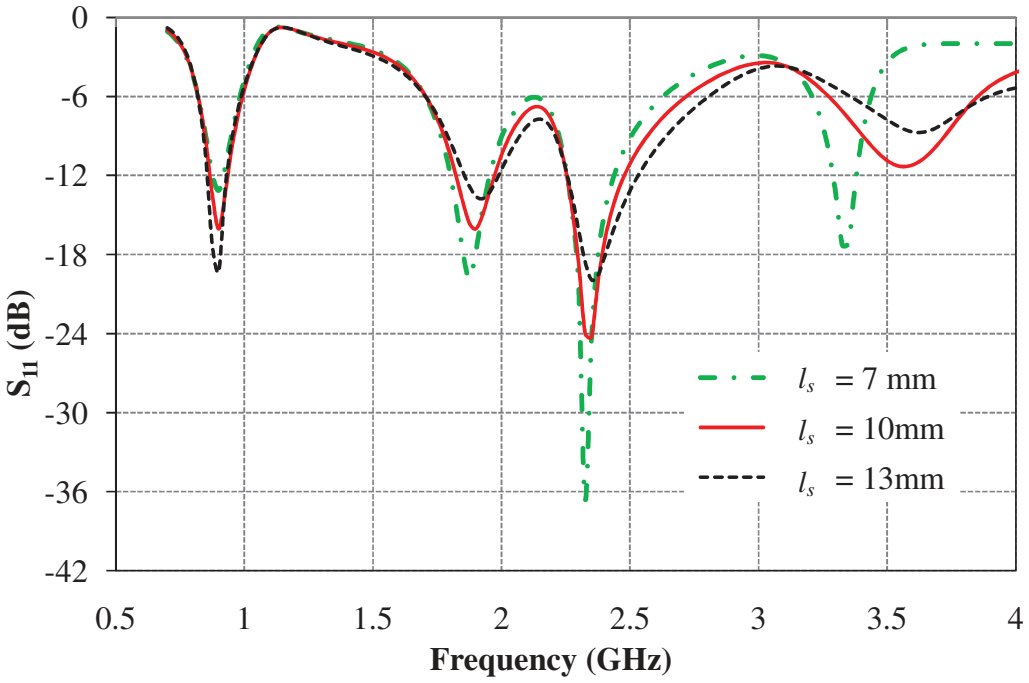

Fig. 4.8: Variation of reflection coefficient with frequency for length l_s.

4.3.1.2 Measurement of S-parameter

A prototype of the optimized antenna is fabricated using T-Tech QC5000 micro-milling machine. The characteristics of the fabricated prototypes are measured with the help of Anritsu VNA Master MS2038C. The simulated results of HFSS are compared with the simulated results of CST MWS and measured results of the antenna operating in free space. Variation of reflection coefficient of the proposed antenna with frequency in free space is shown in Fig. 4.9. It is observed that the proposed antenna covers GSM850/900 (0.820 GHz – 0.970 GHz), GSM1800/GSM1900/UMTS/Wi-Fi/LTE2300/2500 (1.7 GHz – 2.72 GHz), and WIMAX (3.3 GHz – 3.9 GHz). The simulated results are in good agreement with measured results. Some discrepancies are observed due to manufacturing tolerances and surrounding objects (as measurement is not done in anechoic chamber).

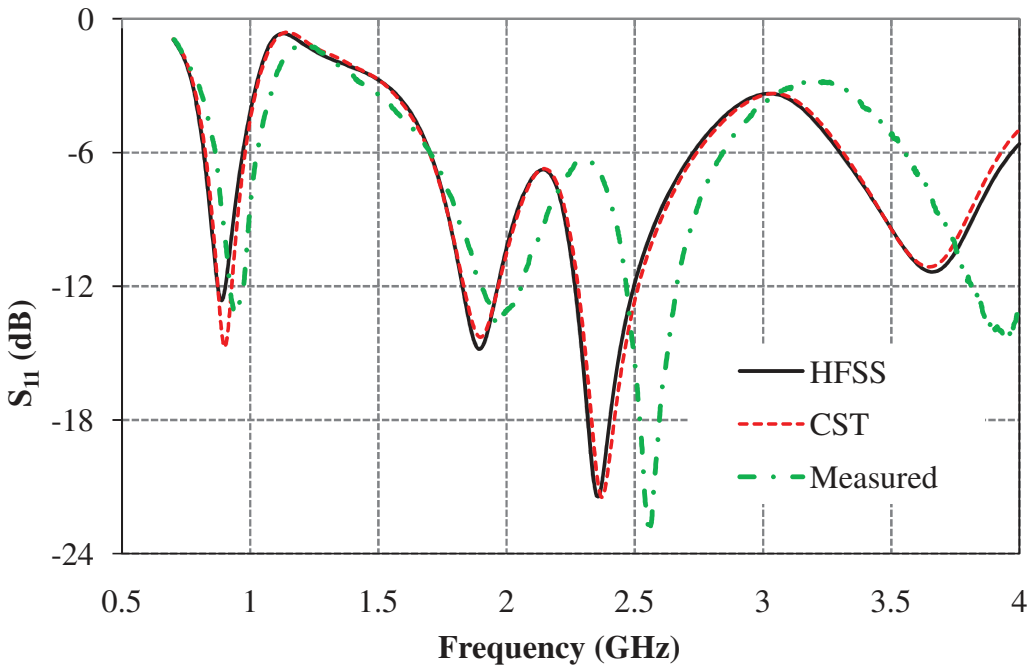

Fig. 4.9: Simulated and measured reflection coefficient of the proposed antenna.

4.3.2 Surface Current Distributions

Further to understand the radiation mechanism of the proposed antenna surface current distributions at different frequencies (0.925 GHz, 1.925 GHz, 2.45 GHz, and 3.5 GHz) are plotted which are shown in Fig 4.10. It is observed that at 0.925 GHz the maximum current is concentrated along the meandered line section and shorted strip sections which are responsible for maximum radiation. When the frequency increases the C-shaped strip starts radiating along with another branch which is also clear from the current distribution plot. At 1.925 GHz, 2.45 GHz, and 3.5 GHz the surface current is distributed on all the branches of the antenna with respect to corresponding electrical lengths therefore, for radiation on these frequency all the branches are responsible which is also clear from Fig. 4.2.

4.3.3 Far Field Radiation Characteristics

The radiation characteristics of proposed antenna in three principal planes are shown in Fig. 4.11. It can be seen that, dumbbell like shape in XY- and YZ-plane of the E_θ-component and close to omni-directional pattern in XZ- plane for the 0.925 GHz, 1.925 GHz, 2.45 GHz, and 3.5 GHz frequencies. In addition, the E_θ-component of the field is dominant and provides smooth variations over all the θ angles which can be seen in XZ-plane as shows in Fig 4.11(a) and 4.11 (c) at 0.925 GHz and 2.45 GHz. This is due to dominant mode is excited at 0.925 GHz and favorable higher order mode is excited at 2.45 GHz, which can be seen from the current distributions on aperture as shown in Fig 4.10 (a) and 4.10 (c), respectively. In YZ-plane, E_φ-component of field is dominant and having almost uniform variations over all φ angles. Comparable E_θ and E_φ components are seen in all the three principal planes resulting into elliptical polarization. In mobile application, there is a significance of total field rather than one component, so even though the vertical component variation is not uniform, an addition of both the vertical and horizontal component gives the fairly good angular coverage.

The measure peak realized gain and simulated total radiation efficiency variation with frequency are plotted in Fig 4.12. It is observed that the peak realized gain is lies between 1.6–1.8 dBi, 2.5–4.2 dBi, and 1.2–3.7 dBi

corresponding to GSM850/GSM900, 1.7 GHz–2.72 GHz, and WiMAX bands, respectively. It is also observed that the total radiation efficiency varies from 60 – 93% in the operating bands.

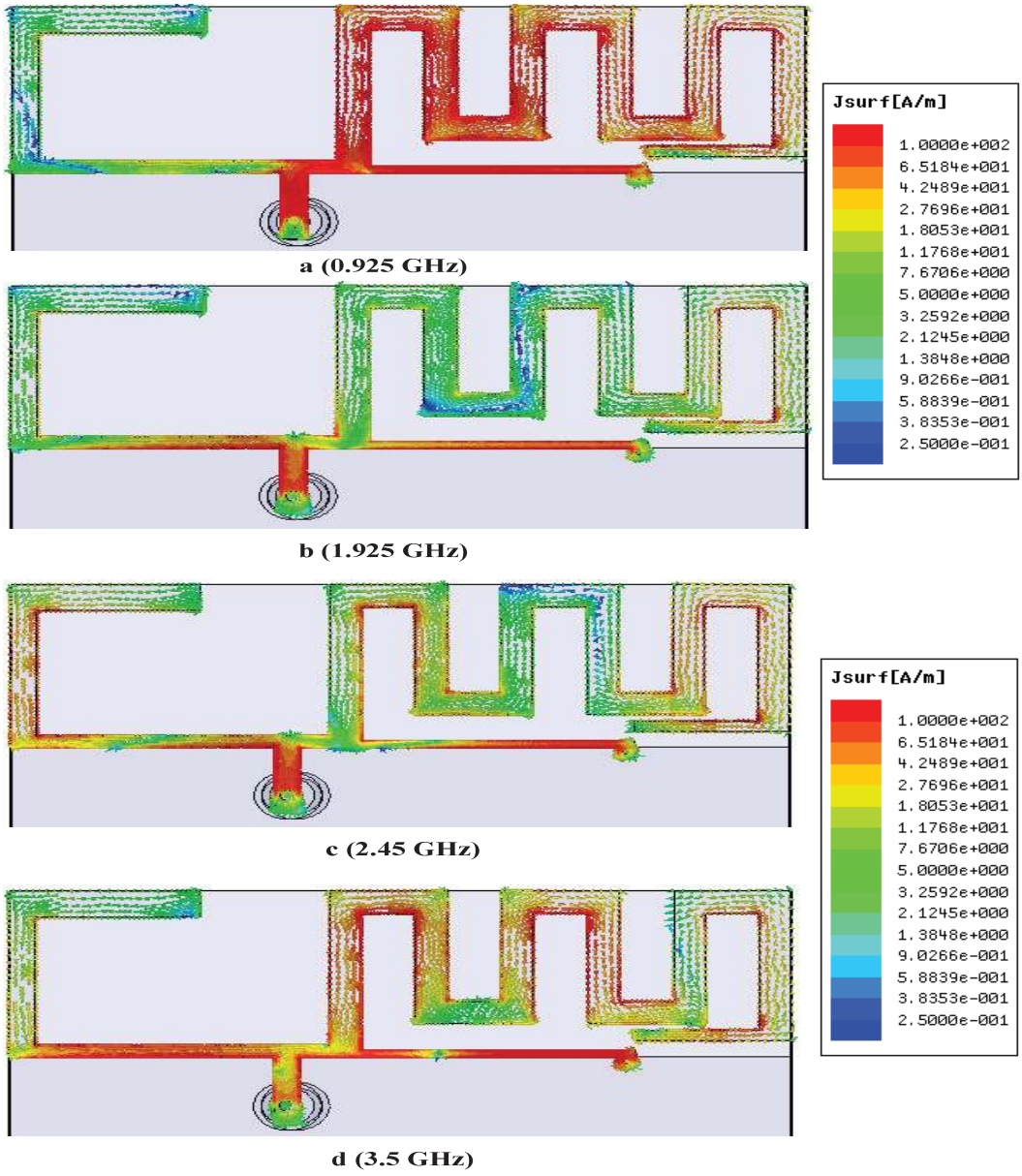

Fig. 4.10: Surface current distributions at different frequencies.

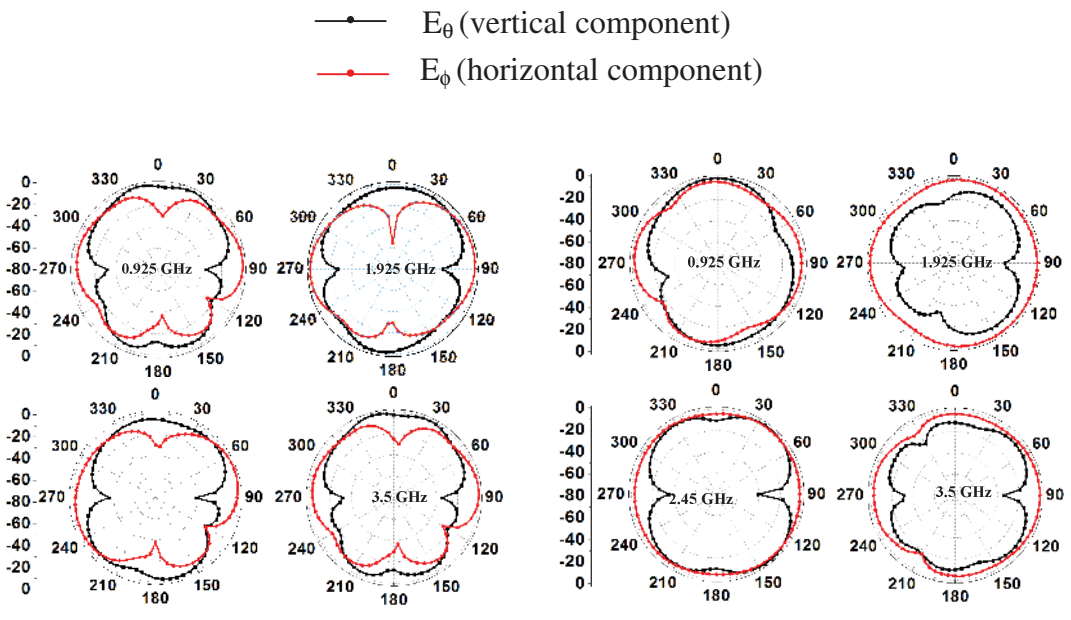

(a)

X-Y Plane (Theta = 90^o and Phi = all)

(b)

Y-Z Plane(Theta = all and Phi =90^o)

(c)

X-Z Plane(Theta = all and Phi =0)

Fig. 4.11: Measured radiation patterns at different frequencies.

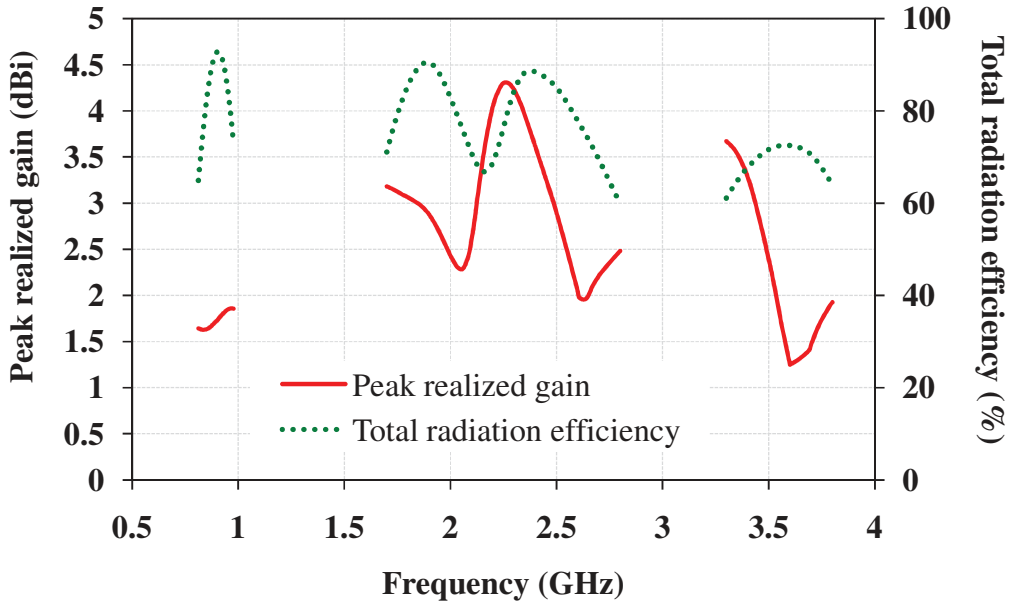

Fig. 4.12: Variation of measured peak realized gain and calculated total radiation efficiency with frequency.

4.4 Antenna Characterization in Mobile Environment

The proposed antenna is also investigated in vicinity of the mobile environment. Mobile environment is made of different component like PCB, plastic housing, LCD, and battery. The dimensions of plastic housing, LCD display, and battery are chosen 60×120×14.3 mm^3, 48×80×2 mm^3, and 33.5×50.5×4 mm^3, respectively. A setup is designed in Ansoft (HFSS) as shown in Fig 4.13. The battery and LCD display are assumed as PEC (Perfect Electric Conductor) material. Battery is placed on the antenna side whereas LCD display placed on ground side. Both are placed 1 mm far from the substrate. Battery and LCD are connected to the substrate with metallic connecting pins provided at the ends of the components. Further, the positions of connecting pins which connect the LCD or battery to the PCB are also a critical parameter to be analyzed. Therefore, different cases of connecting pins positions are studied like when connecting pins are placed toward antenna side only, far from the antenna side, and when the connecting pins are placed at the both ends of the components. The

variation of reflection coefficient with frequency for mobile environment with different positions of connecting pins and antenna in free space are shows in Fig 4.14. It is observed that resonating bands are slightly shifted towards lower frequency side for both the lower and higher frequency bands in all the cases. Less significant effect is observed on the overall impedance matching. Therefore, it can be concluded that there is no significant effect observed on the performance of the antenna in the mobile environment.

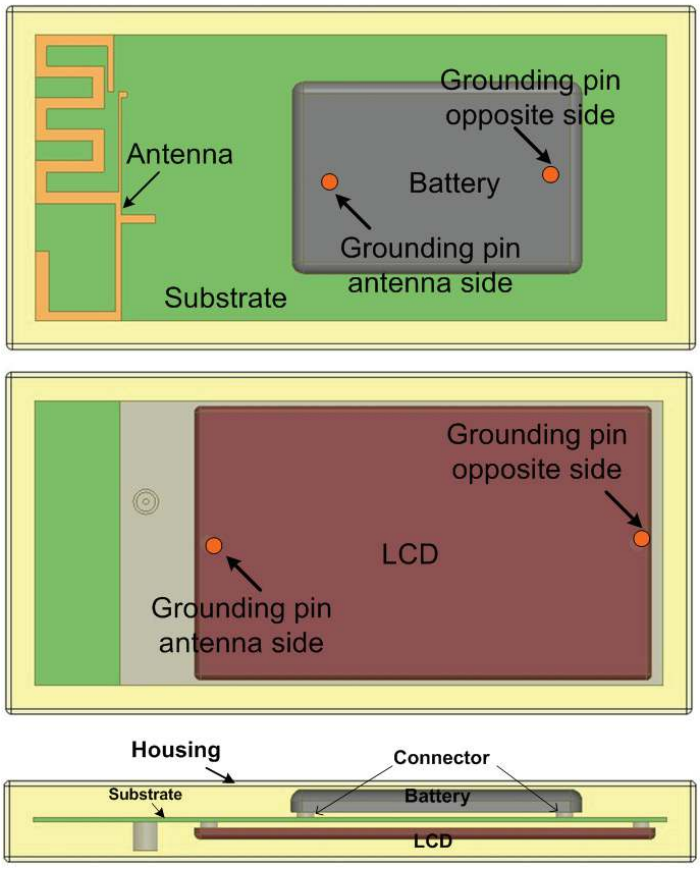

Fig. 4.13: Antenna in mobile environment.

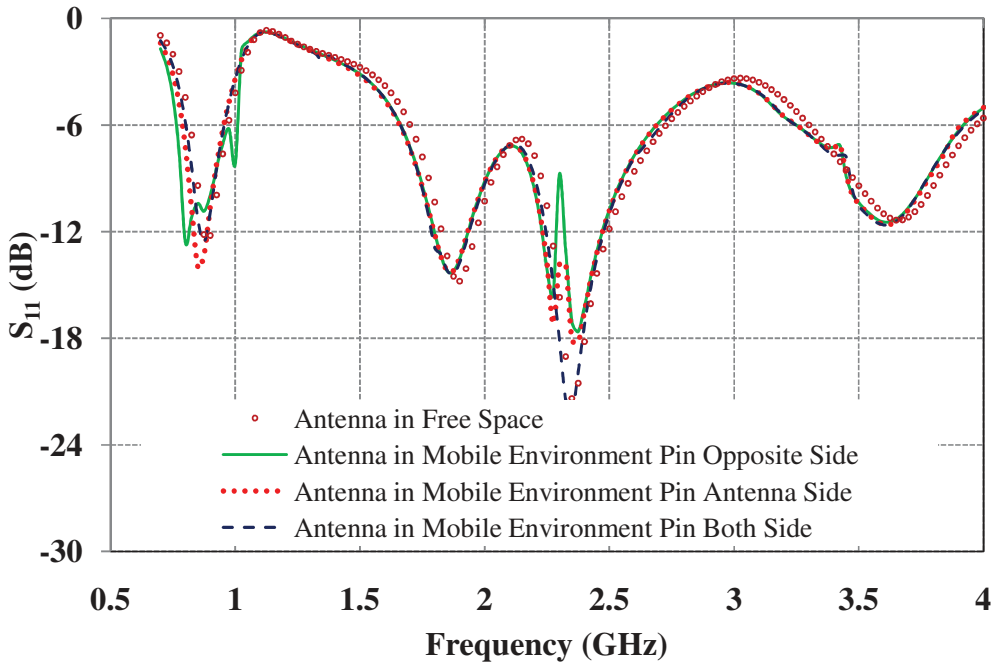

Fig. 4.14: Effect of mobile environment on S-parameters.

Having completed the study on multiband shorted monopole antenna for handset applications, the investigations on thin profile wideband printed monopole antenna for slim mobile handsets applications is carried out in the next chapter.